International Communications in Heat and Mass Transfer 35 (2008) 1275–1280

Contents lists available at ScienceDirect

International Communications in Heat and Mass Transfer

journal homepage: www.elsevier.com/locate/ichmt

MHD-conjugate heat transfer analysis for a vertical flat plate in presence of viscous dissipation and heat generation ☆

A.A. Mamun [a,*], Z.R. Chowdhury [b], M.A. Azim [c], M.M. Molla [d]

[a] Institute of Natural Sciences, United International University, Dhaka-1209, Bangladesh
[b] Department of Electrical and Electronic Engineering, United International University, Dhaka-1209, Bangladesh
[c] School of Business Studies, Southeast University, Dhaka, Bangladesh
[d] Department of Mechanical Engineering, University of Glasgow, Glasgow G12 8QQ, UK

ARTICLE INFO

Available online 8 November 2008

Keywords:
Magnetohydrodynamic
Conjugate heat transfer
Viscous dissipation
Heat generation
Vertical flat plate
Finite difference

ABSTRACT

In this paper, the effects of magnetic field, viscous dissipation and heat generation on natural convection flow of an incompressible, viscous and electrically conducting fluid along a vertical flat plate in the presence of conduction are investigated. Numerical solutions for the governing momentum and energy equations are given. A discussion is provided for the effects of magnetic parameter, viscous dissipation parameter and heat generation parameter on two-dimensional flow. Detailed analysis of the velocity profile, temperature distribution, skin friction, rate of heat transfer and the surface temperature distribution are shown graphically.

1. Introduction

The natural convection flow of an incompressible, viscous and electrically conducting fluid has been studied by several research groups [1–5] due to its potential application in nuclear reactors' cooling system design. In these studies the wall conduction resistance for the convective heat transfer between a solid wall and a fluid flow was neglected considering a thin vertical wall. However, in practical systems the wall conduction resistances have a significant effect in the fluid flow and in the heat transfer characteristics in the vicinity of the wall. Thus the conduction in the solid wall and the convection in the fluid, known as conjugate heat transfer (CHT), should be determined simultaneously.

Perelman [6] first studied the boundary layer equations for the fluid flow over a flat plate of finite thickness considering two-dimensional thermal conduction in the plate. The investigation was then extended by Luikov et al. [7] and since then various types of CHT problems have been studied. The early theoretical and experimental works of the CHT for a viscous fluid have been reviewed by Gdalevich and Fertman [8] and Miyamoto et al. [9]. Miyamoto observed that a mixed-problem study of the natural convection has to be performed for an accurate analysis of the thermo-fluid-dynamic (TFD) field if the convective heat transfer depends strongly on the thermal boundary conditions. Pozzi and Lupo [10] investigated the entire TFD field resulting from the coupling of natural convection along and conduction inside a heated flat plate by means of two expansions, regular series and asymptotic expansions. Moreover, Vynnycky and Kimura [11] studied the two-dimensional conjugate free convection for a vertical plate of finite extent adjacent to a semi-infinite porous medium using finite difference techniques. Pop et al. [12] extended the analysis of Vynnycky for the mixed convection flow. On the other hand, Hossain [5] studied the effects of viscous dissipation and Joule heating on magneto-hydro-dynamic (MHD) natural convection flow. The equations governing the flow were solved and the numerical solutions were obtained for coolant liquid metals, with small Prandtl number, using Keller box [13] scheme. Vajravelu and Hadjinicolaou [14] analyzed the heat transfer behavior within the boundary layer of a viscous fluid over a stretching sheet with viscous dissipation and internal heat generation. In this analysis, the volumetric rate of heat generation, $q'''[W/m^3]$, was considered as $q'''=Q_0(T-T_\infty)$ for $T \geq T_\infty$ and equal to zero for $T<T_\infty$, where Q_0 is a heat generation constant. This relation is legitimate as an approximation of the condition of some exothermic process having T_∞ as the onset temperature. They used $Q_0(T-T_\infty)$ when the inlet temperature is not less than T_∞. Moreover, effects of heat generation/absorption and thermophoresis on hydromagnetic flow along a flat plate were studied by Chamkha and Camille [15].

This article illustrates the effects of magnetic field and heat generation on the coupling of conduction inside and the laminar natural convection along a flat plate in the presence of viscous dissipation. The effects have not been studied yet, according to the authors' best knowledge. The developed equations representing the effects are converted into the dimensionless equations by using suitable transformations with a goal to attain similarity solutions. The

☆ Communicated by A.R. Balakrishnan and S. Jayanti.

* Corresponding author.
E-mail address: mamun3213ssh@gmail.com (A.A. Mamun).

0735-1933/$ – see front matter © 2008 Elsevier Ltd. All rights reserved.
doi:10.1016/j.icheatmasstransfer.2008.06.007

Nomenclature

b	plate thickness
C_{fx}	local skin friction coefficient
c_p	specific heat at constant pressure
f	dimensionless stream function
g	acceleration due to gravity
H_0	strength of the magnetic field
κ_f, κ_s	fluid and solid thermal conductivities, respectively
l	length of the plate
M	magnetic parameter
N	viscous dissipation parameter
Nu_x	local Nusselt number
Pr	Prandtl number
Q	heat generation parameter
T_b	temperature at outside surface of the plate
T_f	temperature of the fluid
T_s	solid temperature
T_∞	fluid ambient temperature
$\bar{u}$, $\bar{v}$	velocity components
u,v	dimensionless velocity components
$\bar{x}$, $\bar{y}$	Cartesian coordinates
x,y	dimensionless Cartesian coordinates
β	coefficient of thermal expansion
τ_w	shearing stress
μ,ν	dynamic and kinematic viscosities, respectively
ρ	density of the fluid
σ	electrical conductivity

non-dimensional equations are then transformed into non-linear equations by introducing a non-similarity transformation. The resulting non-linear equations, together with their corresponding boundary conditions based on conduction and convection, are solved numerically with the help of the finite difference method along with Newton's linearization approximation. There are emphases on the evolution of the surface shear stress in terms of the local skin friction coefficient and the rate of heat transfer in terms of local Nusselt number. The velocity profiles, temperature distributions within the boundary layer and temperature distributions on the interface are also studied.

2. Mathematical analysis

Let us consider a steady natural convection flow of an electrically conducting, viscous and incompressible fluid along a vertical flat plate of length l and thickness b (Fig. 1). It is assumed that the temperature at the outside surface is maintained at a constant temperature T_b, where $T_b > T_\infty$, the ambient temperature of the fluid. A uniform magnetic field of strength H_0 is imposed along the $\bar{y}$-axis.

The boundary layer equations governing the convective flow under these assumptions with the Boussinesq approximations can be written as

$$\frac{\partial \bar{u}}{\partial \bar{x}} + \frac{\partial \bar{v}}{\partial \bar{y}} = 0 \tag{1}$$

$$\bar{u}\frac{\partial \bar{u}}{\partial \bar{x}} + \bar{v}\frac{\partial \bar{v}}{\partial \bar{y}} = \nu\frac{\partial^2 \bar{u}}{\partial \bar{y}^2} + g\beta(T_f - T_\infty) - \frac{\sigma H_0^2 \bar{u}}{\rho} \tag{2}$$

$$\bar{u}\frac{\partial T_f}{\partial \bar{x}} + \bar{v}\frac{\partial T_f}{\partial \bar{y}} = \frac{\kappa_f}{\rho c_p}\frac{\partial^2 T_f}{\partial \bar{y}^2} + \frac{\nu}{c_p}\left(\frac{\partial \bar{u}}{\partial \bar{y}}\right)^2 + \frac{Q_0}{\rho c_p}(T_f - T_\infty) \tag{3}$$

The Viscous dissipation and heat generation term are included in the energy equation (Eq. (3)). The term $\frac{Q_0}{\rho c_p}(T_f - T_\infty)$, Q_0 being a constant, represents the amount of generated or absorbed heat per unit volume. Heat is generated or absorbed from the source term according as Q_0 is positive or negative.

These governing equations have to be solved along with the following boundary conditions [16–19]

$$\left.\begin{array}{ll} \bar{u} = 0, & \bar{v} = 0 \\ T_f = T(\bar{x}, 0), & \dfrac{\partial T_f}{\partial \bar{y}} = \dfrac{k_s}{b k_f}(T_f - T_b) \end{array}\right\} \text{on } \bar{y} = 0,\ \bar{x} > 0$$
$$\bar{u} \to 0,\ T_f \to T_\infty \text{ as } \bar{y} \to \infty,\ \bar{x} > 0 \tag{4}$$

The non-dimensional governing equations and boundary conditions can be obtained from Eqs. (1–4) using the following non-dimensional quantities [20]

$$x = \frac{\bar{x}}{l}, y = \frac{\bar{y}}{l}Gr^{1/4}, u = \frac{\bar{u}l}{\nu}Gr^{-1/2}, v = \frac{\bar{v}l}{\nu}Gr^{-1/4}$$
$$\frac{T_f - T_\infty}{T_b - T_\infty} = \theta, Gr = \frac{g\beta l^3(T_b - T_\infty)}{\nu^2} \tag{5}$$

where l is the length of the plate, Gr is the Grashof number and θ is the dimensionless temperature.

The non-dimensional governing equations can be written as

$$\frac{\partial u}{\partial x} + \frac{\partial v}{\partial y} = 0 \tag{6}$$

$$u\frac{\partial u}{\partial x} + v\frac{\partial u}{\partial y} + Mu = \frac{\partial^2 u}{\partial y^2} + \theta \tag{7}$$

$$u\frac{\partial \theta}{\partial x} + v\frac{\partial \theta}{\partial y} = \frac{1}{Pr}\frac{\partial^2 \theta}{\partial y^2} + N\left(\frac{\partial u}{\partial y}\right)^2 + Q\theta \tag{8}$$

where $M = \frac{\sigma H_0^2 l^2}{\mu Gr^{1/2}}$ is the magnetic parameter, $N = \frac{\nu^2 Gr}{l^2 c_p (T_b - T_\infty)}$ is the viscous dissipation parameter, $Q = \frac{Q_0 L^2}{\mu c_p Gr^{1/2}}$ is the heat generation parameter and $Pr = \frac{\mu c_p}{\kappa_f}$ is the Prandtl number.

If the length of the plate l is considered to be $\left(\frac{\kappa_f b}{\kappa_s}\right)Gr^{1/4}$, the corresponding boundary conditions are obtained in non-dimensional form as follows:

$$u = 0\ v = 0,\ \theta - 1 = \frac{\partial \theta}{\partial y} \text{ on } y = 0,\ x > 0$$
$$u \to 0,\ \theta \to 0 \text{ as } y \to \infty,\ x > 0 \tag{9}$$

Eqs. (7) and (8) are solved for the above boundary conditions (9). The variables ψ, η and θ are introduced in the following forms to facilitate the solution:

$$\psi = x^{4/5}(1+x)^{-1/20} f(x,\eta)$$
$$\eta = y x^{-1/5}(1+x)^{-1/20}$$
$$\theta = x^{1/5}(1+x)^{-1/5} h(x,\eta) \tag{10}$$

here η is the similarity variable and ψ is the non-dimensional stream function which satisfies the continuity equation and is related to the

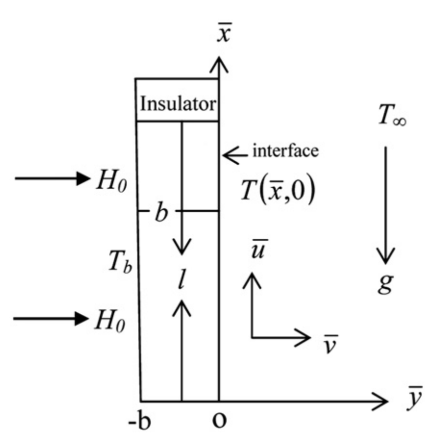

Fig. 1. Physical model and coordinate system.

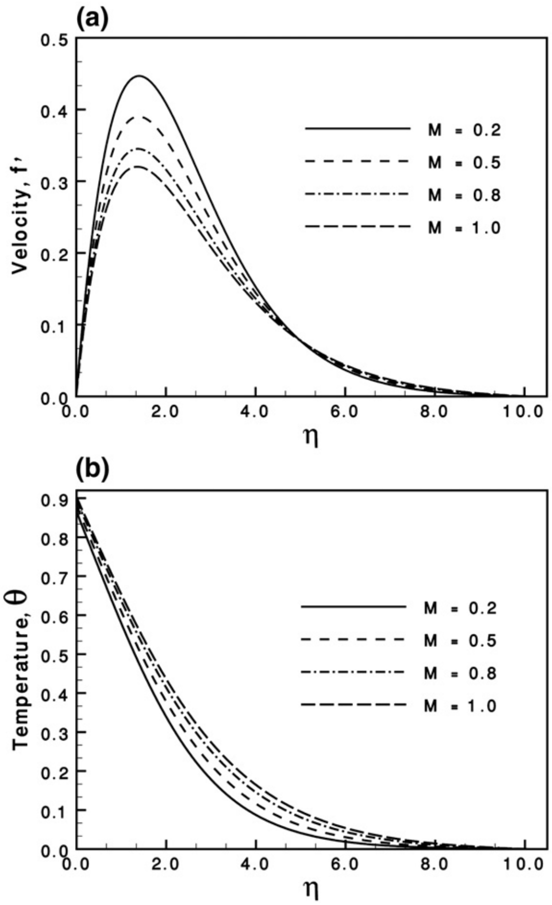

Fig. 2. (a) Variation of velocity profiles and (b) variation of temperature profiles against η for varying of M with $Q=0.01$ and $N=0.01$.

velocity components in the usual way as $u=\partial\psi/\partial y$ and $v=-\partial\psi/\partial x$. Moreover, $h(x,\eta)$ represents the dimensionless temperature. The momentum and energy equations (Eqs. (7) and (8), respectively) are transformed for the new coordinate system. At first, the velocity components are expressed in terms of the new variables for this transformation. Thus we get

$$f''' + \frac{16+15x}{20(1+x)} f f'' - \frac{6+5x}{10(1+x)} f'^2 - Mx^{2/5}(1+x)^{1/10} f' + h = x\left(f'\frac{\partial f'}{\partial x} - f''\frac{\partial f}{\partial x}\right) \tag{11}$$

$$\frac{1}{Pr}h'' + \frac{16+15x}{20(1+x)} f h' - \frac{1}{5(1+x)} f' h + Nx(f'')^2 + Qx^{2/5}(1+x)^{1/10} h = x\left(f'\frac{\partial h}{\partial x} - h'\frac{\partial f}{\partial x}\right) \tag{12}$$

where primes denote differentiation with respect to η. The boundary conditions as mentioned in Eq. (9) then take the following form:

$$\begin{aligned} & f(x,0) = f'(x,0) = 0 \\ & h'(x,0) = -(1+x)^{1/4} + x^{1/5}(1+x)^{1/20} h(x,0) \\ & f'(x,\infty) \to 0, \;\; h(x,\infty) \to 0 \end{aligned} \tag{13}$$

The Eqs. (11) and (12), governing the MHD-conjugate convective heat transfer problems together with the boundary conditions 13 reduce to those analysis of Merkin and Pop [17] if $M=0$, $N=0$, $Q=0$ and $x^{1/5}=\xi$ are considered.

The set of equations, Eqs. (11) and (12), together with the boundary conditions (Eq. (13)) are solved numerically by applying the implicit finite difference method with Keller box scheme [13,21]. It is important from practical point of view to calculate the values of the rate of heat transfer in terms of the Nusselt number and the surface shear stress in terms the skin friction coefficient. These can be written in the non-dimensional form as [20,22]

$$C_f = \frac{Gr^{-3/4} l^2}{\mu \nu}\tau_w \text{ and } Nu = \frac{l Gr^{-1/4}}{\kappa_f (T_b - T_\infty)} q_w \tag{14}$$

where τ_w $[=\mu(\partial\bar{u}/\partial\bar{y})_{\bar{y}=0}]$ and q_w $[=-\kappa_f(\partial T_f/\partial\bar{y})_{\bar{y}=0}]$ are the shearing stress and the heat flux, respectively. Using the new variables described in Eq. (5), Eq. (14) can be written as

$$C_{fx} = x^{2/5}(1+x)^{-3/20} f''(x,0) \tag{15}$$

$$Nu_x = -(1+x)^{-1/4} h'(x,0) \tag{16}$$

The numerical values of the surface temperature are also obtained from the relation

$$\theta(x,0) = x^{1/5}(1+x)^{-1/5} h(x,0) \tag{17}$$

We have also discussed the velocity profiles and the temperature distributions for different values of the magnetic parameter, viscous dissipation parameter and heat generation parameter.

3. Results

The resulting solutions for the velocity profiles and temperature distributions are shown in Figs. 2 and 3. In the simulation, the value of the Prandtl number is considered to be 0.733 that corresponds to hydrogen. Detailed numerical solutions have been obtained for different values of other parameters considered for the analysis.

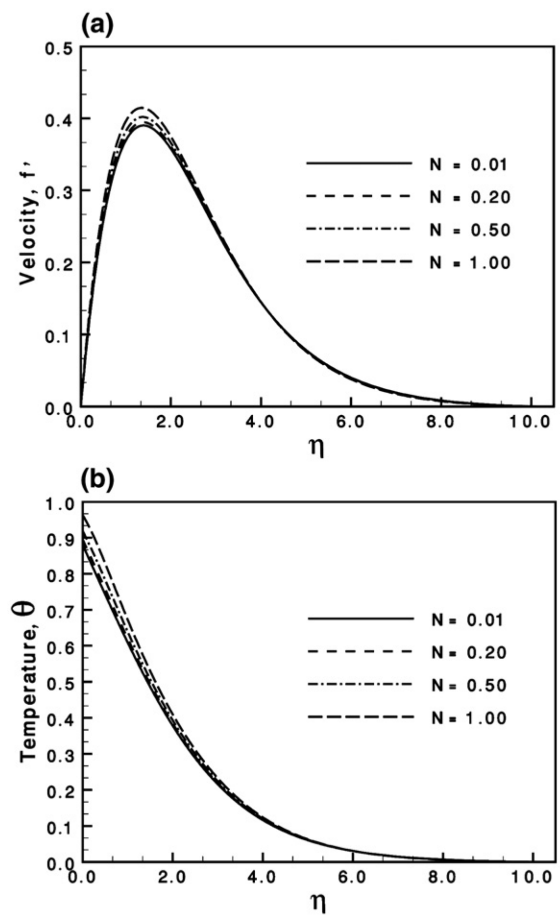

Fig. 3. (a) Variation of velocity profiles and (b) variation of temperature profiles against η for varying of N with $Q=0.01$ and $M=0.5$.

Table 1
Comparison of the present numerical results of surface temperature with Prandtl number $Pr=0.733$ and $M=0$, $N=0$ and $Q=0$

$x^{1/5}=\xi$	$\theta(x,0)$		
	Pozzi and Lupo [10]	Merkin and Pop [17]	Present work
0.7	0.651	0.651	0.651
0.8	0.684	0.686	0.687
0.9	0.708	0.715	0.716
1.0	0.717	0.741	0.741
1.1	0.699	0.762	0.763
1.2	0.640	0.781	0.781

Table 2
Comparison of the present numerical results of skin friction coefficient with Prandtl number $Pr=0.733$ and $M=0$, $N=0$ and $Q=0$

$x^{1/5}=\xi$	C_{fx}		
	Pozzi and Lupo [10]	Merkin and Pop [17]	Present work
0.7	0.430	0.430	0.424
0.8	0.530	0.530	0.529
0.9	0.635	0.635	0.635
1.0	0.741	0.745	0.744
1.1	0.829	0.859	0.860
1.2	0.817	0.972	0.975

A comparison of the surface temperature and the local skin friction factor obtained in the present work with $x^{1/5}=\xi$, $M=0$, $N=0$, and $Q=0$ and obtained by Pozzi and Lupo [10] and Merkin and Pop [17] have been shown in Tables 1 and 2, respectively. It is evident that there is an excellent agreement among the respective results.

The magnetic parameter M, representing the Lorentz force, opposes the flow. The peak velocity decreases with the increasing M due to this retarding effect as shown in Fig. 2(a). As a result, the separation of the boundary layer occurs earlier since the momentum boundary layer becomes thicker.

From Fig. 2(b) it can be observed that the magnetic field decreases the temperature gradient at the wall and increases the temperature in the flow region for a particular value of η. Thus, the magnetic parameter increases the thickness of the thermal boundary layer. Temperature at the interface also varies since the conduction is considered within the plate.

Fig. 3(a) and (b) illustrates the variation of the velocity and temperature profiles with η for selected values of N when $M=0.5$, and $Q=0.01$. It can be noted from Fig. 3(a) that an increase in the viscous dissipation parameter N is associated with a slight increase in the velocity. This behavior is similar to that of temperature profile as shown in Fig. 3(b). It implies that the viscous dissipation enhances the temperature and therefore increases the velocity.

Fig. 4 displays the numerical results of the velocity and temperature, respectively obtained from the solution of the Eqs. (11) and (12) subject to the boundary condition 13 for different small values of Q plotted against η with $M=0.5$, and $N=0.01$. The velocity gradient at the surface increases due to the increasing Q and accordingly, the velocity of the fluid increases as shown in Fig. 4(a). It is observed from Fig. 4(a) that for each value of the heat generation parameter there exists a global maximum of the velocity within the boundary layer. The maximum velocities are 0.3215, 0.3382, 0.3512 and 0.3600 for $Q=0.01$,0.05, 0.08, and 0.10, respectively. It can be seen that the velocity increases by 10.694% as Q increases from 0.01 to 0.10.

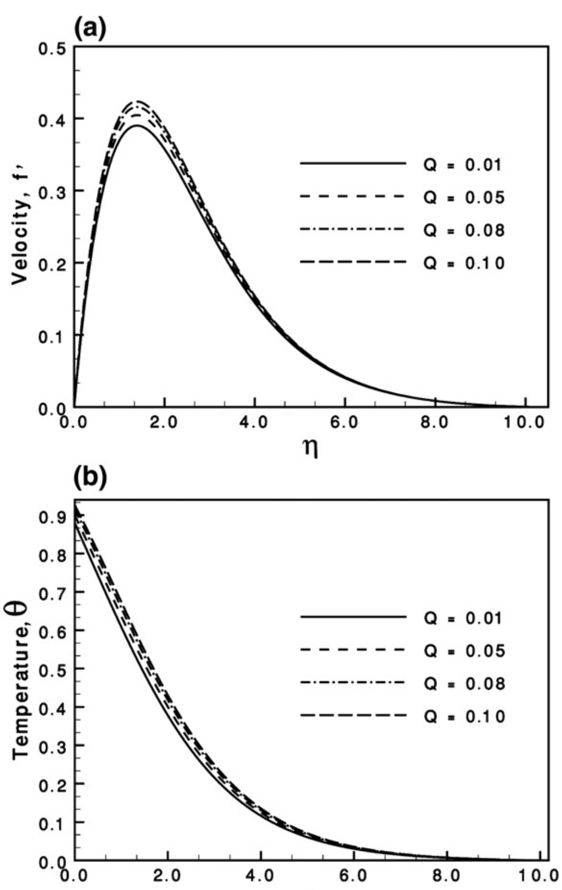

Fig. 4. (a) Variation of velocity profiles and (b) variation of temperature profiles against η for varying of Q with $M=0.5$ and $N=0.01$.

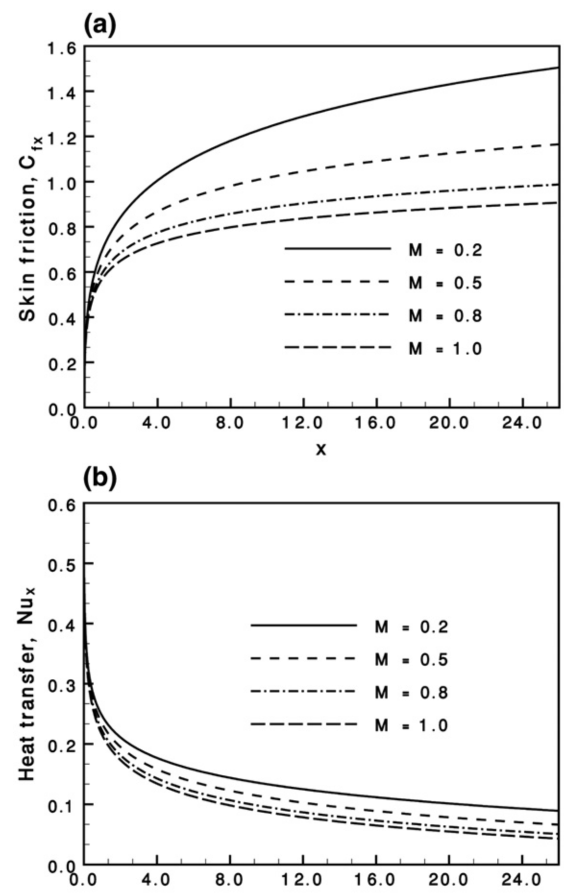

Fig. 5. (a) Variation of skin friction coefficients and (b) variation of rate of heat transfer against x for varying of M with and $N=0.01$ and $Q=0.01$.

Fig. 4(b) presents clearly that the temperature increases gradually for increasing Q and exceeds the level of the surface temperature. As a result there exists critical levels of temperature near the interface which therefore decreases the level of local Nusselt number (see Fig. 7(b)).

The variation of the local skin friction coefficient C_{fx} and local rate of heat transfer Nu_x with $N=0.01$ and $Q=0.01$ for different values of M at different positions are illustrated in Fig. 5. The Magnetic force opposes the flow, as mentioned earlier, and reduces the shear stress at the wall. The reduced skin friction coefficients with the increasing M represent this phenomenon as illustrated in Fig. 5(a). Moreover, the heat transfer rate depends on the gradient of temperature. As the gradient decreases with the increasing M [Fig. 2(b)], the heat transfer rate also decreases as revealed in Fig. 5(b).

Fig. 6(a) and (b) illustrates the effect of viscous dissipation parameter on the local skin friction coefficient and the local heat transfer rate, respectively while $M=0.50$, and $Q=0.01$. It can be seen that the skin friction factor increases with an increase in the viscous parameter. Moreover, the skin friction coefficient increases along the x direction for a particular N. This is to be expected since the fluid motion within the boundary layer increases for increasing N (Fig. 3(b)) and eventually increases the skin friction factor. Fig. 6(b) shows that the effect of the viscous parameter leads to a decrease of the local heat transfer rate. i.e. the greater value of N, the lower heat transfer rate.

Fig. 7(a) and (b) plots the local skin friction coefficient and the local heat transfer rate against x for different values of heat generation parameter Q in the presence of viscous magnetic field. It can be concluded that an increase in the heat generation parameter leads to an increase in the skin friction factor and a decrease in the local heat transfer rate. The increasing Q accelerates the fluid flow, as mentioned

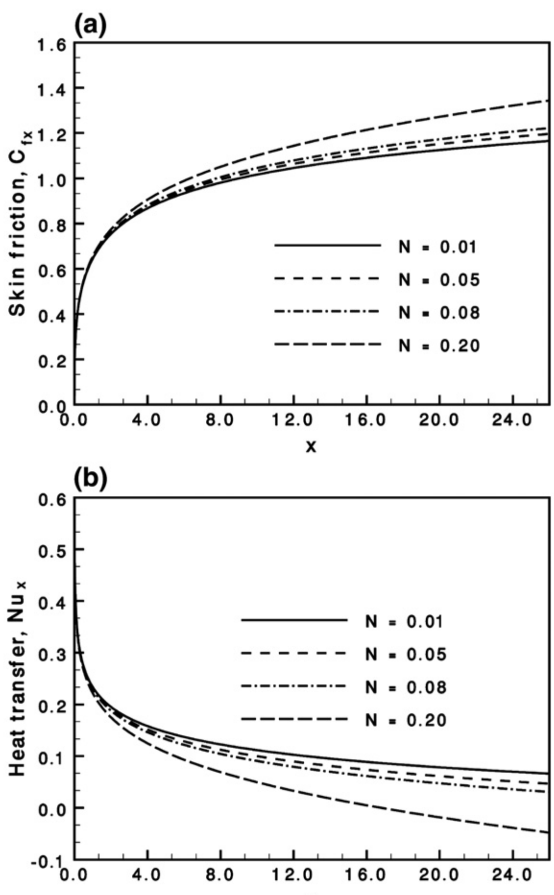

Fig. 6. (a) Variation of skin friction coefficients and (b) variation of rate of heat transfer against x for varying of N with $M=0.5$ and $Q=0.01$.

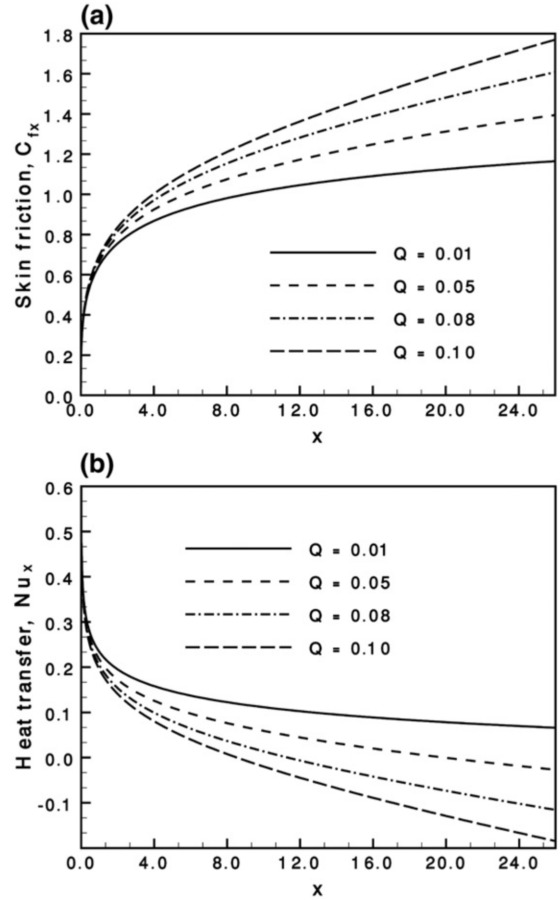

Fig. 7. (a) Variation of skin friction coefficients and (b) variation of rate of heat transfer against x for varying of Q with $M=0.5$ and $Q=0.01$.

in Fig. 4(a), and generates the greater bouyancy force and therefore increases the skin friction factor. On the other hand, owing to the increasing Q, there creates a hot layer of fluid near the surface. As a result the resultant temperature of the fluid exceeds the surface temperature. Accordingly, the rate of heat transfer from the surface decreases.

Fig. 8(a) and (b) illustrates the influence of the magnetic parameter M and the viscous dissipation parameter N on interfacial temperature with x. It is seen that the interfacial temperature rises along the x direction for a particular value of M. Moreover, the increasing M gives rise to an increased solid-fluid interface temperature. This is expected behaviour since the magnetic field acting along the horizontal direction increases the temperature as observed in Fig. 2(b). On the other hand, it can be revealed that the interfacial temperature increases with increasing x for a given value of N. Higher values of N result in a greater temperature variation on the wall compared with the case of lower value of N.

Fig. 9 presents the variation of the surface temperature distribution as a function of x for different values of Q. It can be noted that the interfacial temperature increases with increasing x for a particular value of Q. Furthermore, the temperature at the interface increases for the increasing Q. This is because the temperature within the boundary layer increases for the increasing Q as observed in Fig. 4(b).

4. Conclusion

A time independent, two-dimensional, laminar free convection flow is studied considering conduction, viscous dissipation and heat generation in the presence of a magnetic field. The dimensionless boundary layer equations together with the corresponding boundary

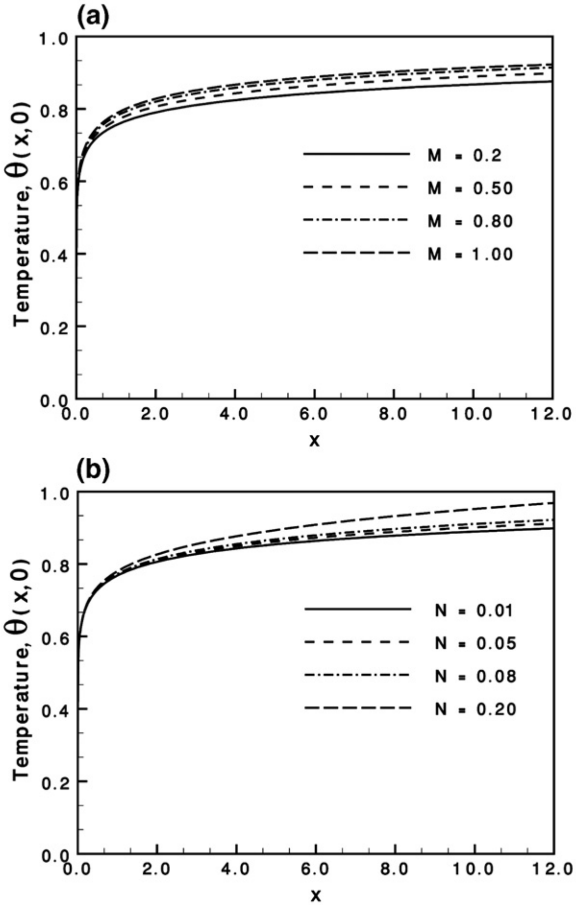

Fig. 8. (a) Variation of surface temperature distributions against x for different values of M with N=0.01 and Q=0.01 and (b) Variation of surface temperature distributions against x for different values of N with M=0.5, and Q=0.01.

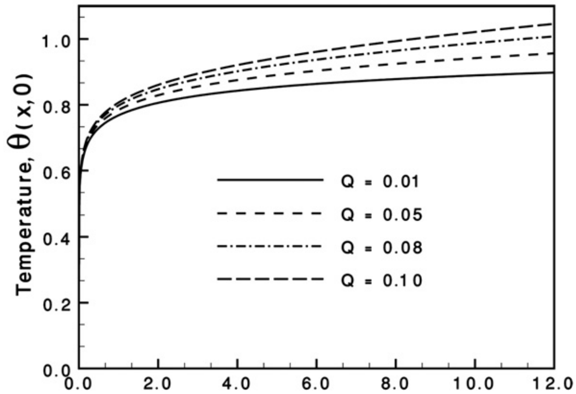

Fig. 9. Variation of surface temperature distributions against x for different values of Q with M=0.5 and N=0.01.

conditions are solved numerically using implicit finite difference method. The effects of the magnetic field, dissipation parameter and heat generation parameter are analyzed on the fluid flow. The velocity of the fluid and the skin friction at the interface increase with the decreasing magnetic field while they decrease with the decreasing dissipation parameter and heat generation parameter. The temperature of the fluid increases with the increasing magnetic field, dissipation parameter and heat generation parameter. Moreover, the rate of heat transfer decreases with the increasing magnetic field, dissipation parameter and heat generation parameter. The surface temperature increases with the increasing magnetic parameter, dissipation parameter and heat generation parameter.

References

[1] E.M. Sparrow, R.D. Cess, Effect of magnetic field on free convection heat transfer, Int. J. Heat Mass Transfer 3 (1961) 267–274.
[2] K.R. Sing, T.G. Cowling, Thermal conduction in magnetohydrodynamics, J. Mech. Appl. Math. 16 (1963) 1–5.
[3] N. Riley, Magnetohydrodynamic free convection, J. Fluid Mech. 18 (1964) 577–586.
[4] H.K. Kuiken, Magnetohydrodynamic free convection in strong cross flow field, J. Fluid Mech. 40 (1970) 21–38.
[5] M.A. Hossain, Viscous and joule heating effects on MHD-free convection flow with variable plate temperature, Int. J. Heat Mass Transfer 35 (1992) 3485–3487.
[6] T.L. Perelman, On conjugated problems of heat transfer, Int. J. Heat Mass Transfer 3 (1961) 293–303.
[7] A.V. Luikov, V.A. Aleksashenko, A.A. Aleksashenko, Analytical methods of solution of conjugated problems in convective heat transfer, Int. J. Heat Mass Transfer 14 (1971) 1047–1056.
[8] L.B. Gdalevich, V.E. Fertman, Conjugate problems of natural convection, Inzh-Fiz. Zh. 33 (1977) 539–547.
[9] M. Miyamoto, J. Sumikawa, T. Akiyoshi, T. Nakamura, Effects of axial heat conduction in a vertical flat plate on free convection heat transfer, Int. J. Heat Mass Transfer 23 (1980) 1545–1553.
[10] A. Pozzi, M. Lupo, The coupling of conduction with laminar natural convection along a flat plate, Int. J. Heat Mass Transfer 31 (1988) 1807–1814.
[11] M. Vynnycky, S. Kimura, Transient conjugate free convection due to a heated vertical plate, Int. J. Heat Mass Transfer 39 (1996) 1067–1080.
[12] I. Pop, D. Lesnic, D.B. Ingham, Conjugate mixed convection on a vertical surface in a porous medium, Int. J. Heat Mass Transfer 38 (1995) 1517–1525.
[13] H.B. Keller, Numerical methods in the boundary layer theory, Annu. Rev. Fluid Mech. 10 (1978) 417–433.
[14] K. Vajravelu, A. Hadjinicolaou, Heat transfer in a viscous fluid over a stretching sheet with viscous dissipation and internal heat generation, Int. Commun. Heat Mass Transfer 20 (1993) 417–430.
[15] A.J. Chamkha, I. Camille, Effects of heat generation/absorption and the thermophoresis on hydromagnetic flow with heat and mass transfer over a flat plate, Int. J. Numer. Methods Heat Fluid Flow 10 (2000) 432–448.
[16] A.K. Luikov, Conjugate convective heat transfer problems, Int. J. Heat Mass Transfer 16 (1974) 257–265.
[17] J.H. Merkin, I. Pop, Conjugate free convection on a vertical surface, Int. J. Heat Mass Transfer 39 (1996) 1527–1534.
[18] I. Pop, D.B. Ingham, Convective Heat Transfer: Mathematical and Computational Modeling of Viscous Fluids and Porous Media, Pergamon, Oxford, 2001, p. 179.
[19] C.L. Chang, Numerical simulation of micropolar fluid flow along a flat plate with wall conduction and buoyancy effects, J. Appl. Phys. D 39 (2006) 1132–1140.
[20] M.M. Molla, M.A. Hossain, M.A. Taher, Magnetohydrodynamic natural convection flow on a sphere with uniform heat flux in presence of heat generation, Acta Mech. 186 (2006) 75–86.
[21] T. Cebeci, P. Bradshaw, Physical and Computational Aspects of Convective Heat Transfer, Springer, New York, 1984.
[22] M.M. Molla, M.A. Taher, M.M.K. Chowdhury, M.A. Hossain, Magnetohydrodynamic natural convection flow on a sphere in presence of heat generation nonlinear analysis, Modell. Control 10 (4) (2005) 349–363.